Evaluation of moving-coil loudspeaker and passive radiator parameters using normal-incidence sound transmission measurements: Theoretical developments[a)]

Timothy W. Leishman[b)] and Brian E. Anderson
Acoustics Research Group, Department of Physics and Astronomy, Brigham Young University, N283 Eyring Science Center, Provo, Utah 84602

(Received 25 October 2012; revised 14 March 2013; accepted 16 April 2013)

The parameters of moving-coil loudspeaker drivers are typically determined using direct electrical excitation and measurement. However, as electro-mechano-acoustical devices, their parameters should also follow from suitable mechanical or acoustical evaluations. This paper presents the theory of an acoustical method of excitation and measurement using normal-incidence sound transmission through a baffled driver as a plane-wave tube partition. Analogous circuits enable key parameters to be extracted from measurement results in terms of open and closed-circuit driver conditions. Associated tools are presented that facilitate adjacent field decompositions and derivations of sound transmission coefficients (in terms of driver parameters) directly from the circuits. The paper also clarifies the impact of nonanechoic receiving tube terminations and the specific benefits of downstream field decompositions. © *2013 Acoustical Society of America*.
[http://dx.doi.org/10.1121/1.4803900]

PACS number(s): 43.38.Ja, 43.20.Ye, 43.20.Mv, 43.55.Rg [DDE] Pages: 223–236

NOMENCLATURE

B = Magnetic flux density in the magnet air gap
c = Speed of sound in air
c_d = Speed of sound in the downstream tube air
C_{MS} = Mechanical compliance of the driver suspension
c_p = Specific heat for air
c_u = Speed of sound in the upstream tube air
d = Depth of the porous receiving-tube termination
d_m = Microphone separation distance in the two-microphone transfer-function technique
$\hat{e}_g$ = Complex open-circuit voltage amplitude of a signal generator
f = Frequency
f_0 = *In vacuo* resonance frequency of the driver diaphragm and suspension system
$j = \sqrt{-1}$
k = Acoustic wave number
$\tilde{k}$ = Complex acoustic wave number (accounting for propagation losses) in the plane wave tubes
$\tilde{k}'_m$ = Complex acoustic wave number within the termination material
l = Effective length of the voice-coil conductor in the magnet air gap
L_d = Length of the receiving tube
L_E = Effective electric inductance of the driver voice coil
M_{MD} = Effective mechanical mass of the driver diaphragm assembly without fluid loading
$\hat{p}(x)$ = Complex acoustic pressure amplitude at a point x in a one-dimensional sound field
$\langle\hat{p}(x)\rangle_S$ = Cross-sectional spatially averaged complex acoustic pressure amplitude at a point x in a one-dimensional sound field
$\hat{p}_d$ = Complex amplitude of the total acoustic pressure on the downstream face of a device under test
$\langle\hat{p}_d\rangle_S$ = Spatially averaged total complex pressure amplitude on the downstream face of a device under test
$\hat{p}_{d,i}$ = Complex amplitude of the acoustic pressure incident upon the receiving tube at the downstream face of a device under test
$\hat{p}_{d,r}$ = Complex amplitude of the acoustic pressure reflected from the receiving tube at the downstream face of a device under test
$\hat{p}_i$ = Complex amplitude of the acoustic pressure incident upon a device under test
$\hat{p}_i(x)$ = Complex amplitude of the incident acoustic pressure at a point x in a one-dimensional sound field
$\hat{p}_u$ = Complex amplitude of the total acoustic pressure on the upstream face of a device under test
$\langle\hat{p}_u\rangle_S$ = Spatially averaged total complex pressure amplitude on the upstream face of a device under test
Pr = Prandtl number for air
$\hat{p}_r(x)$ = Complex amplitude of the reflected acoustic pressure at a point x in a one-dimensional sound field
$\hat{p}_t$ = Complex amplitude of the acoustic pressure transmitted past a device under test
$\langle\hat{p}_{TH}\rangle_S$ = Cross-sectional spatially averaged Thevenin equivalent acoustic pressure

[a)]Portions of this work were presented in "Derivation of moving-coil loudspeaker parameters using acoustical testing techniques: Theoretical developments," 145th Meeting of the Acoustical Society of America, Nashville, TN, April 2003 and "An acoustical measurement method for the derivation of loudspeaker parameters," 115th Convention of the Audio Engineering Society, New York, October 2003.
[b)]Author to whom correspondence should be addressed. Electronic mail: tim_leishman@byu.edu

$\hat{p}_{u,i}$ = Complex amplitude of the acoustic pressure incident upon a device under test from the upstream side

$\hat{p}_{u,r}$ = Complex amplitude of the acoustic pressure reflected from the upstream face of a device under test

$R(x)$ = Complex pressure-amplitude reflection coefficient at a point x in a one-dimensional sound field

R_{ATT} = Acoustic resistance of the receiving tube termination after being translated to the magnet and frame (or diaphragm) of the driver under test

$R_{ATT,LF}$ = Acoustic resistance of the receiving tube termination in the low-frequency limit after being translated to the magnet and frame (or diaphragm) of the driver under test

R_E = DC electric resistance of the driver voice coil

R_g = Internal electric resistance of a signal generator

R_{MS} = Mechanical resistance of the driver suspension

R_T = Complex pressure-amplitude reflection coefficient of the receiving-tube termination

S = Inside cross-sectional area of the plane-wave tubes

S_d = Inside cross-sectional area of the downstream plane-wave tube

S_D = Effective cross-sectional area of the driver diaphragm

S_u = Inside cross-sectional area of the upstream plane-wave tube

TL = Transmission loss

$\hat{u}(x)$ = Complex particle velocity amplitude at a point x in a one-dimensional sound field

$\langle \hat{u}(x) \rangle_S$ = Cross-sectional spatially averaged complex particle velocity amplitude at a point x in a one-dimensional sound field

$\hat{U}(x)$ = Complex volume velocity amplitude at a point x in a one-dimensional sound field

$\hat{U}_d$ = Complex volume velocity amplitude at the downstream face of a device under test

$\hat{U}_D$ = Complex volume velocity produced by the driver diaphragm

$\hat{U}_u$ = Complex volume velocity amplitude at the upstream face of a device under test

$\langle W_i \rangle_t$ = Time-averaged sound power incident upon a device under test

$\langle W_t \rangle_t$ = Time-averaged sound power transmitted past a device under test

X_{ATT} = Acoustic reactance of the receiving tube termination after being translated to the magnet and frame (or diaphragm) of the driver under test

$X_{ATT,LF}$ = Acoustic reactance of the receiving tube termination in the low-frequency limit after being translated to the magnet and frame (or diaphragm) of the driver under test

X_E = Electric reactance of the driver voice coil

X_M = Mechanical reactance of the driver diaphragm and suspension

$X_{M,HF}$ = Mechanical reactance of the driver diaphragm and suspension in the high-frequency limit

$X_{M,LF}$ = Mechanical reactance of the driver diaphragm and suspension in the low-frequency limit

Z_A = Acoustic impedance

$Z_A(x)$ = Acoustic impedance at a point x in a one-dimensional sound field

$Z_{A,d}$ = Acoustic impedance looking into the receiving tube from the downstream face of a device under test

$Z_{A,i}(x)$ = "Incident" component of the acoustic impedance at a point x in a one-dimensional sound field

$Z_{A,r}(x)$ = "Reflected" component of the acoustic impedance at a point x in a one-dimensional sound field

Z_{AT} = Acoustic impedance of the receiving tube termination

Z_{ATH} = Thevenin equivalent acoustic impedance

Z_{ATT} = Acoustic impedance of the receiving tube termination after being translated to the magnet and frame of the driver under test, $= Z'_{ATT}$ if the magnet and frame of the driver are acoustically unobtrusive

Z'_{ATT} = Acoustic impedance of the receiving tube termination as seen by the driver diaphragm, $= Z_{ATT}$ if the magnet and frame of the driver under test are acoustically unobtrusive

$Z_{A,u}$ = Acoustic impedance looking into the upstream face of a device under test from the source tube

Z_E = Internal blocked electric impedance of the driver voice coil

Z_{ET} = Electric impedance inserted between the driver terminals for a specific test condition

Z_M = Mechanical impedance, mechanical impedance of the driver diaphragm and suspension

$Z_S(x)$ = Specific acoustic impedance at a point x in a one-dimensional sound field

$Z_{S,a}$ = Apparent specific acoustic impedance

α_p = Total propagation absorption (attenuation) coefficient in the plane-wave tubes

α_T = Absorption coefficient of the receiving tube termination

β = Substitution in the formulations of X_E

γ = Ratio of specific heats for air

η = Coefficient of shear viscosity for air

κ = Thermal conductivity for air

Ξ' = Specific flow resistance of the termination material

ρ_0 = Ambient density of air

ρ_d = Ambient density of air in the downstream tube

ρ_u = Ambient density of air in the upstream tube

ω = Angular frequency, $= 2\pi f$

σ = Porosity of the termination material

τ = Sound transmission coefficient

τ_{CC} = Sound transmission coefficient when the driver terminals are closed circuited

τ_{OC} = Sound transmission coefficient when the driver terminals are open circuited

$\tau_{OC,0}$ = Sound transmission coefficient at resonance when the driver terminals are open circuited

τ_{SL} = Sound transmission coefficient of an ideal single-leaf partition (or open-circuit loudspeaker), with cross-sectional area $S_D = S$

I. INTRODUCTION

Many methods have been devised over the years to measure the properties of moving-coil loudspeaker drivers. They are often expressed in terms of Thiele–Small or related parameters to facilitate efficient modeling and design of complete loudspeaker systems.[1–10] Their assessment typically involves some form of direct electrical excitation or measurement, or both. However, because drivers are electro-mechano-acoustical devices, they should also lend themselves to parameter evaluations through appropriate mechanical or acoustical excitation and measurement. Since these latter approaches have not been fully developed, this paper takes a step to address the deficiency by introducing the theory of plane-wave tube sound transmission measurements of drivers, enabling their parameters to be determined through acoustical excitation and measurement alone.

Currently, the most common methods of evaluating small-signal driver parameters involve multi-step mechanical or acoustic perturbations of electric impedance measurements taken at driver terminals. The moving mass and suspension compliance of a driver are determined from resonance frequencies evaluated with and without the perturbations in place. The added-mass technique, discussed by Beranek[11] and others, requires a known, appreciable mass to be carefully attached to a diaphragm with appropriate distribution and driver orientation. The closed-box technique, discussed by Thiele[1] and others, requires the use of an airtight box with a known enclosed volume after a driver has been mounted to it. Both approaches can be time consuming and problematic in implementation, with relative bias errors often reaching 10% or higher.[12,13]

The parameters may also be determined through alternative means, such as simultaneous measurement of dissimilar dynamic signals. Christophorou proposed the simultaneous measurement of electric impedance and diaphragm velocity (via a mounted accelerometer).[14] Others employed laser velocity transducers to measure diaphragm velocities or microphones to measure enclosed or near-field acoustic pressures.[15–18] Each involved transfer functions between an electric input signal and a measured mechanical or acoustic output signal. Optimization techniques have also been developed to derive small-signal parameters from isolated electric impedance measurements.[19–24] Despite the potentials of all these methods, the perturbation techniques are still widely used, likely because of their ubiquity and the persistence of traditional methods, or the fact that they are relatively simple (not requiring specialized equipment or computer programming).

Because the various techniques require electric signals applied to driver voice coils or electrical measurements taken at driver terminals, or both, the mechanical parameters are determined through the tacit assumption that the electromagnetic force factor (Bl product) has been accurately determined. However, the latter can depend significantly upon diaphragm displacement, with relative measurement bias errors also tending to be high.[12,13] The measured mechanical parameters may thus become contaminated through the use of electric signals and measurement techniques. Furthermore, electric impedance measurements can suffer contamination from environments that are acoustically noisy or that fail to meet free-field conditions.[11,14,21] They also suffer from random errors that often require repeated assessments to yield acceptable parameter values.[13]

Several authors have explored variations of loudspeaker parameters over common diaphragm excursion ranges.[25–27] Clark proposed a useful electric impedance-based measurement system to assess parameters with static pressure displacing a driver diaphragm from equilibrium.[16] His approach included six methods to determine the position-dependent suspension compliance. One did not require the application of an electric signal to the voice coil, but instead involved acoustic excitation of the driver mounted on the wall of a test chamber by another loudspeaker inside. A transfer function was then evaluated using the near-field acoustic pressure outside the chamber as the output. While the method thus involved a form of sound transmission through the driver, it did not quantify the transmission in a definitive sense. Instead, its purpose was simply to estimate the resonance frequencies of the system under various diaphragm displacements and from them determine the position-dependent suspension compliance.

While additional background could be offered,[13] the foregoing should enable one to appreciate the significance of the approach presented in this paper. It is based on the well-known fact that acoustic properties of materials (e.g., acoustic impedances, reflection coefficients, absorption coefficients, transmission coefficients, etc.) may be conveniently determined when they are measured as terminations to or partitions between plane-wave tubes. Particularly efficient methods of assessment involve the two-microphone transfer function technique,[28–33] which decomposes adjacent one-dimensional sound fields into incident and reflected components to yield the acoustic characteristics of interest. It stands to reason that the properties of a moving-coil driver might likewise be assessed under similar circumstances (i.e., when mounted as a termination to a plane-wave tube or a partition between adjacent plane-wave tubes). They could also be assessed when the driver is configured with different electrical conditions (e.g., with terminals open or closed circuited). Because such electric perturbations are consistent, easily controlled, and automated without mechanically disturbing the driver, this special application of plane-wave tube measurements should provide an important and useful option in the practical characterization of drivers.

The idea for the method stemmed from work in the field of active sound transmission control involving loudspeakers as actuators in active segmented partitions.[34–37] While underlying theoretical and experimental tools were developed to assess normal-incidence transmission losses and other properties of partitions using plane-wave tubes, the evaluation of loudspeaker driver parameters was not part of the effort. Some of the established concepts were later applied to loudspeaker measurements,[13,38] but without sufficient development or explanation. The purpose of this paper is then to formally present, expand, and clarify the analytical tools needed to derive common parameters from the normal-incidence sound transmission through a driver, while

exploring key methodological capabilities and limitations. The sound transmission coefficient or transmission loss is of particular interest because it does not require knowledge of an exact driver diaphragm location (i.e., its effective acoustic position) in the plane-wave tube system to produce acceptable values.

As part of the development, the paper introduces a useful method to decompose one-dimensional sound fields represented by analogous circuits into forward and backward-propagating components. This enables efficient modeling of sound transmission through general electro-mechano-acoustical devices, including but not limited to loudspeaker drivers. It also enhances the understanding of plane-wave tube measurement effects, including those associated with nonanechoic terminations and downstream field decompositions.

The method presented herein is not intended to replace tools currently available to measure driver parameters, but to complement them. It differs in kind from these tools in the sense that it employs both acoustical excitation and measurement. It enables frequency-dependent characterization of key mechanical properties without measurement errors introduced by inaccurate or inconsistent electromagnetic driver parameters. These properties include the isolated mechanical impedance Z_M of the driver diaphragm and suspension, its *in vacuo* resonance frequency f_0, the mechanical resistance R_{MS} of the suspension, the moving mass M_{MD} of the diaphragm assembly (independent of fluid loading), and the mechanical compliance C_{MS} of the driver suspension. The method also offers a theoretical alternative to the measurement of electromagnetic driver parameters, including the Bl product, the electric reactance X_E of the voice coil, and the effective electric inductance L_E of the voice coil. Other small-signal parameters may be derived from these properties. The method can easily overcome the effects of ambient noise and does not require three-dimensional free-field conditions.

The approach could serve as a valuable diagnostic tool in the evaluation of malfunctioning drivers or those found to have abnormal parameter values via electrical testing. Because it requires no externally applied electric voice-coil signals or electrical measurements, it is also well suited for the evaluation of passive radiator parameters. This may be one of its most important advantages, as methods for measuring the mechano-acoustic properties of fully assembled passive radiators are ostensibly lacking.

This paper accordingly introduces a specialized method of loudspeaker driver and passive radiator parameter measurements, and a means whereby values determined from electrical measurements may be substantiated. The following sections explore the approach through analogous circuit modeling and associated parameter derivations from sound transmission coefficients. The consequences of nonanechoic downstream tube terminations and downstream field decompositions are also clarified through theoretical analysis and numerical examples.

II. ANALOGOUS CIRCUITS

The proposed measurement method is based on the system depicted in Fig. 1 (see the nomenclature section for clarifications). From left to right, it includes (1) an excitation source with arbitrary internal impedance, (2) an upstream (source) tube, (3) a partition consisting of the driver under test in a rigid baffle, (4) a downstream (receiving) tube, and (5) a receiving tube termination of arbitrary acoustic impedance Z_{AT}. The driver under test is assumed to have an open basket or frame (typical of most low-frequency and full-range drivers), so sound can transmit effectively through it. Flush-mounted microphones are positioned at least one effective tube diameter away from the closest tube end.[32] The microphones in each pair are spaced a distance d_m

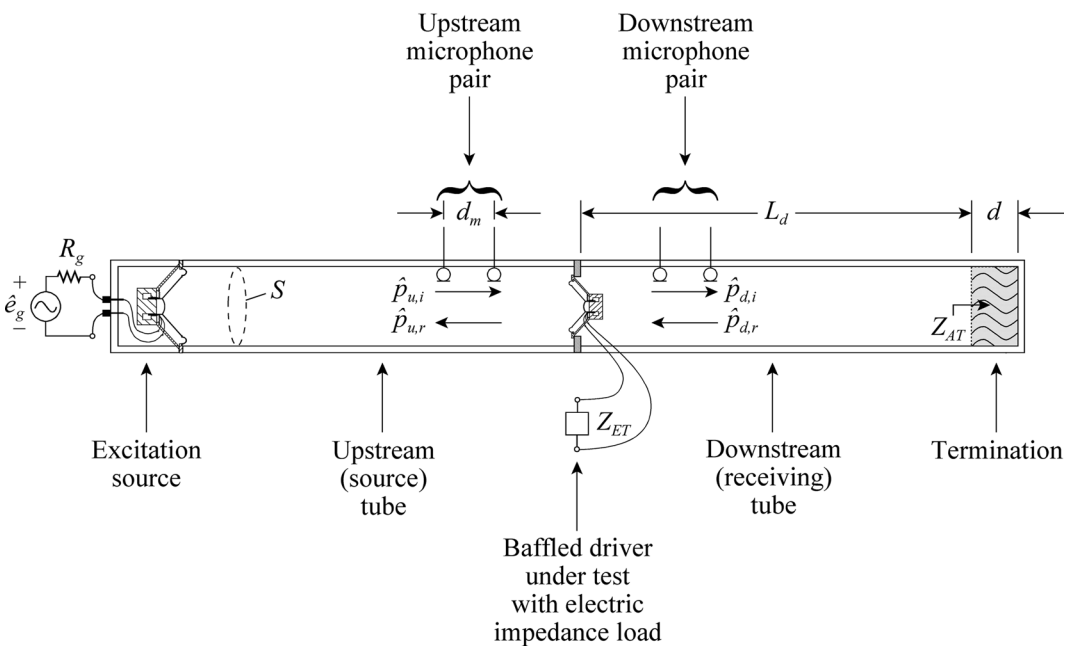

FIG. 1. Diagram of the proposed plane-wave tube transmission loss measurement system for the evaluation of loudspeaker driver parameters.

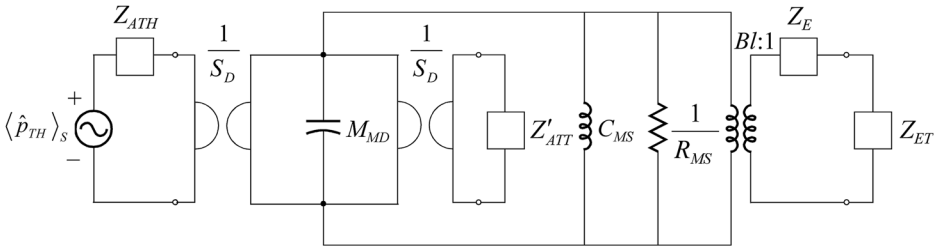

FIG. 2. Multiple-domain analogous circuit representing a moving-coil loudspeaker driver under test in a plane-wave tube transmission loss measurement system. Several circuit reduction steps have already been implemented as described in the text.

from one another following the bandwidth guideline $0.05(c/d_m) \lesssim f \lesssim 0.4(c/d_m)$ to prevent excessive measurement error in the two-microphone transfer function technique.[31] Additional microphones may be introduced to provide other spacings and spliceable measurement data that extend the bandwidth from the lowest frequency of interest to the cutoff frequency of the first tube cross mode. These spacings and the required source and termination section lengths govern the overall length of the system. While a single system may be used to measure many different drivers, its dimensions must ultimately depend upon the requirements of those drivers. The following section discusses the modeling of the system, one part at a time.

A. Measurement system modeling

In practice, the excitation source is a moving-coil loudspeaker itself, which may be adequately modeled using a classical analogous circuit.[11] The circuit is connected to a network representing the upstream plane-wave tube.[39] However, the resulting combination of the two sections may be modeled more succinctly with a Thevenin equivalent circuit. The latter then connects to a network representing the baffled driver under test, which in turn connects to a network representing the downstream tube. The leftmost portion of the downstream tube involves a varying cross-sectional area caused by the presence of the baffle opening, driver frame, magnet, etc. The various constrictions might be modeled using a series of plane-wave-tube circuits with varying cross-sectional areas.[40] However, these and other effects near the driver might be represented more generally through a two-port network.[41] The portion of the tube beyond the frame and magnet structure would again be modeled using a one-dimensional plane-wave tube network connected to the acoustic termination impedance Z_{AT}. For further simplification, an impedance Z_{ATT} could represent the termination impedance translated through the downstream tube to the plane immediately adjacent to the driver structure.[41] Once this impedance is carried through the constriction two-port network, it represents the receiving-space impedance Z'_{ATT} seen by the driver diaphragm. The downstream field is typically probed to the right of that network.

The diaphragm may generally be considered to have a smaller effective area S_D than the cross-sectional areas S of the source and receiving tubes. Its coupling to the tube fields may be modeled to a first approximation (i.e., in the long-wavelength limit) using simple area gyrators with gyration constants $1/S_D$. (The transitions between the smaller and larger areas could be modeled more accurately using junction impedances,[41] but they are neglected here for clarity.)

Many analogous driver circuits have been proposed over the years, but we here employ a classical model in conjunction with the area gyrators to represent the baffled driver under test. For passive tests, an arbitrary electric impedance Z_{ET} would be inserted between the driver terminals to create a specific test condition. It would thus combine in series with the internal blocked electric impedance Z_E of the voice coil. For the open-circuit case, $Z_{ET} \to \infty$, while for the closed-circuit case, $Z_{ET} \to 0$. Other conditions, including active conditions, could also be considered as perturbations.

The driver circuit is combined with elements representing other portions of the measurement system as shown in Fig. 2. To simplify the representation, one may begin by pulling elements through the transformer and gyrators to the acoustic impedance domain. If the driver frame and magnet structure are assumed to be acoustically unobtrusive, the circuit reduces to the acoustic impedance representation of Fig. 3, with $Z'_{ATT} = Z_{ATT} = R_{ATT} + jX_{ATT}$. (Measurements have suggested that this assumption is reasonable for many drivers and frequencies of interest.[36,37])

To reduce the circuit even further, the mechanical driver parameters may be combined into a single mechanical impedance $Z_M = R_{MS} + j(\omega M_{MD} - 1/\omega C_{MS}) = R_{MS} + jX_M$. In addition, the transmission loss of an electro-mechano-acoustic filter should be independent of its effect on the excitation source and upstream field (behaving as a filter in isolation).[42] As a result, the Thevenin equivalent circuit may be replaced (for convenience in theoretical sound-transmission formulations) with another equivalent circuit representing a constant-incident-pressure source and a semi-infinite source tube. If these changes are made, the complete circuit reduces

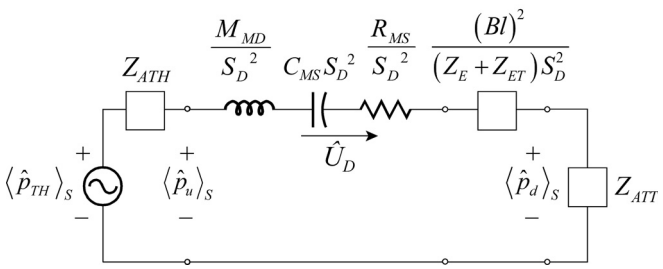

FIG. 3. Acoustic impedance circuit representing a moving-coil loudspeaker driver in a plane-wave tube transmission loss measurement system. Acoustic filtering caused by constrictions of the loudspeaker frame and magnet structure has been neglected.

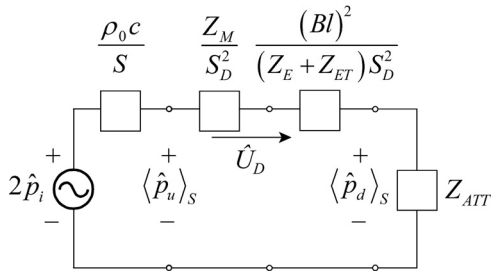

FIG. 4. Simplified acoustic impedance circuit representing a passive moving-coil loudspeaker driver in a plane-wave tube transmission loss measurement system. The upstream tube has been replaced with a constant-incident-pressure source and a semi-infinite tube for convenience in calculations.

to the form shown in Fig. 4. As described later, these circuits enable one to establish useful relationships between the sound transmission through the baffled driver and its parameters.

In Figs. 2–4, the total acoustic pressures are expressed as spatially averaged quantities. At some point x in the upstream or downstream field, the cross-sectional distributions of the total complex acoustic pressure $\hat{p}(x)$, particle velocity $\hat{u}(x)$, and specific acoustic impedance $Z_S(x)$ may not be uniform in what is normally considered a one-dimensional system. Even if a rigid-walled tube is excited below its first cross-mode cutoff frequency, a nonuniform source, termination, or obstruction may produce cross-sectional field nonuniformities. However, because evanescent higher-order modes typically decay out over short distances, only plane waves propagate along the greater length of the tube. In addition, evanescent modes do not contribute appreciably to the complex volume velocity.[41] The propagating plane-wave component extrapolated to a point of nonuniformity has a complex pressure amplitude equivalent to the cross-sectional spatially averaged pressure at that point.[41,43] At a sufficient distance from the irregularity (e.g., one effective tube diameter away[32]), it is therefore possible to ignore the transitional region and treat the former as a vibrating piston with cross-sectional uniformity.[43] In reality, this distance depends upon the desired level of evanescent mode attenuation, the analysis frequency, and its proximity to the cutoff frequency of the first cross mode. As the analysis frequency approaches the cutoff frequency, the distance must be increased to maintain the attenuation.

For general axial positions, it is appropriate to substitute spatially averaged acoustic quantities $\langle \hat{p}(x) \rangle_S$ and $\langle \hat{u}(x) \rangle_S$, and the *apparent* (not spatially averaged) specific acoustic impedance $Z_{S,a} = Z_A S = Z_M / S$ for their local counterparts. In the following analysis, we drop the angled brackets denoting spatial averaging (in essence assuming cross-sectional uniformity) with the understanding that cross-sectional spatial averages provide the most favorable general descriptions for the plane-wave tube system. In the acoustic impedance analogy, spatially averaged pressure and volume velocity are the preferred variables for potential and flow, respectively.

B. One-dimensional wave decomposition

As developments in this section will show, one-dimensional sound fields associated with electro-mechano-acoustical systems may be readily separated into forward and backward propagating wave components. This enables one to conveniently deduce acoustic pressures incident upon, reflected from, and transmitted past points of interest. While traditional analytical formulations of this sort are often cumbersome or impractical for complicated systems (like that described herein), analogous circuit representations can greatly simplify the work.

Suppose a one-dimensional sound field exists in a region adjacent to one or more electro-mechano-acoustical devices in a system. The acoustic impedance $Z_A(x)$ and either the total acoustic pressure $\hat{p}(x)$ or volume velocity $\hat{U}(x)$ are also known at a position x in the field. The incident and reflected acoustic pressures $\hat{p}_i(x)$ and $\hat{p}_r(x)$ may be easily derived from these quantities. To see this, one first writes the total acoustic pressure as

$$\begin{aligned}\hat{p}(x) &= \hat{p}_i(x) + \hat{p}_r(x) = \hat{p}_i(x)\left[1 + \frac{\hat{p}_r(x)}{\hat{p}_i(x)}\right] \\ &= \hat{p}_i(x)[1 + R(x)] = \hat{p}_i(x)\left\{1 + \left[\frac{Z_A(x) - \frac{\rho_0 c}{S}}{Z_A(x) + \frac{\rho_0 c}{S}}\right]\right\} \\ &= 2\hat{p}_i(x)\left[\frac{Z_A(x)}{Z_A(x) + \frac{\rho_0 c}{S}}\right], \end{aligned} \tag{1}$$

where $R(x)$ is the complex pressure-amplitude reflection coefficient evaluated at the position x, ρ_0 is the ambient density of air, and c is the speed of sound. It follows that

$$\hat{p}_i(x) = \frac{\hat{p}(x)}{2}\left[1 + \frac{\rho_0 c}{Z_A(x) S}\right] \tag{2}$$

and

$$\hat{p}_r(x) = \frac{\hat{p}(x)}{2}\left[1 - \frac{\rho_0 c}{Z_A(x) S}\right]. \tag{3}$$

Because the total pressure is the sum of the incident and reflected pressures, the problem may be represented in analogous circuit form as shown in Fig. 5, where $Z_A(x)$ is partitioned into two components corresponding to the two pressure components as $Z_A(x) = Z_{A,i}(x) + Z_{A,r}(x)$. In this case,

$$Z_{A,i}(x) = \frac{Z_A(x) + \frac{\rho_0 c}{S}}{2} \tag{4}$$

and

$$Z_{A,r}(x) = \frac{Z_A(x) - \frac{\rho_0 c}{S}}{2}. \tag{5}$$

From the circuit diagram it is also clear that

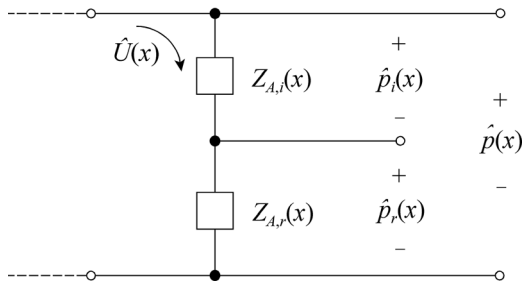

FIG. 5. Acoustic impedance circuit showing the decomposition of incident and reflected acoustic pressure at a point x in a one-dimensional acoustical section of an electro-mechano-acoustical system. At this point, the acoustic impedance is partitioned into two components as $Z_A(x) = Z_{A,i}(x) + Z_{A,r}(x)$.

$$\hat{p}_i(x) = \hat{U}(x) Z_{A,i}(x) = \frac{\hat{U}(x)}{2}\left[Z_A(x) + \frac{\rho_0 c}{S}\right] \tag{6}$$

and

$$\hat{p}_r(x) = \hat{U}(x) Z_{A,r}(x) = \frac{\hat{U}(x)}{2}\left[Z_A(x) - \frac{\rho_0 c}{S}\right]. \tag{7}$$

Hence, using only basic information readily available from an analogous circuit, it is possible to decompose the total acoustic pressure at a given field point into forward and backward-propagating components in a straightforward manner. This saves considerable effort in mathematical analysis and computation, and is particularly beneficial for intricate systems involving multiple physical domains (i.e., acoustical, mechanical, and electrical). Moreover, because of the widespread availability of numerical circuit analysis tools, it facilitates rapid evaluation of even very complicated systems. The following section demonstrates how the approach simplifies the prediction of normal-incidence sound transmission through an electro-mechano-acoustical device.

C. General prediction of normal-incidence sound transmission

Transmission loss (TL) is a key measure in the prediction and evaluation of sound transmission through acoustic filters, materials, mufflers, partitions, and other elements. It is typically defined as

$$\mathrm{TL} = 10 \log_{10}\left(\frac{1}{\tau}\right), \tag{8}$$

where τ is the sound-power transmission coefficient, defined as the ratio of time-averaged sound power transmitted through the device $\langle W_t \rangle_t$ to the time-averaged sound power incident upon it $\langle W_i \rangle_t$.[41,44] It quantifies sound-reducing properties as though they were independent of excitation sources and source spaces. Transmission loss analyses often assume constant incident pressure fields and anechoic transmitting fields.[42,45]

Normal-incidence transmission loss is an important specific measure. If one assumes normal plane-wave propagation on either side of an electro-mechano-acoustical device under test, τ may be characterized as

$$\tau = \frac{\langle W_t \rangle_t}{\langle W_i \rangle_t} = \frac{\rho_u c_u S_d}{\rho_d c_d S_u} \frac{|\hat{p}_t|^2}{|\hat{p}_i|^2}, \tag{9}$$

where $\rho_u c_u$ and $\rho_d c_d$ are the characteristic fluid impedances of the upstream (source) and downstream (receiving) fields, respectively, and S_u and S_d are their cross-sectional areas. Because the adjacent fields may be separated into forward and backward-propagating components as described earlier, it is a straightforward matter to predict the transmission loss using analogous circuits. However, if a constant incident pressure source is used as in Fig. 4, there is no need to decompose the upstream field.

Consider an arbitrary passive, active, or active/passive device (black box) separating a source space and receiving space, as depicted in Fig. 6. The acoustic impedance looking directly into the upstream face of the box is $Z_{A,u}$. The acoustic impedance looking into the receiving tube from its downstream face is $Z_{A,d}$. The (spatially averaged) total acoustic pressures on the two faces are represented by $\hat{p}_u$ and $\hat{p}_d$, respectively, while the corresponding volume velocities are $\hat{U}_u$ and $\hat{U}_d$. The acoustic pressure incident upon the box and that transmitted past the box (i.e., the acoustic pressure incident upon the receiving space) are then solved using Eq. (6) with appropriate upstream and downstream values. Substituting the resulting expressions into Eq. (9) yields the following normal-incidence sound transmission coefficient:

$$\tau = \frac{\rho_u c_u S_d}{\rho_d c_d S_u}\left|\frac{\hat{U}_d}{\hat{U}_u}\right|^2 \left|\frac{Z_{A,d} + \dfrac{\rho_d c_d}{S_d}}{Z_{A,u} + \dfrac{\rho_u c_u}{S_u}}\right|^2. \tag{10}$$

The volume velocity ratio in this expression is advantageous because in the solution of simultaneous circuit loop equations, Cramer's rule typically produces denominators for the volume velocities that are identical. In some cases, the volume velocities themselves are identical. As a result, the ratio often leads to simpler mathematical representations. In addition, $Z_{A,u}$ generally incorporates $Z_{A,d}$ in some fashion. This may lead to further simplifications and clarify how the receiving space termination impedance affects the calculated transmission loss of the black box. Nevertheless, as mentioned earlier, one usually assumes that receiving spaces are free fields such that $Z_{A,d} = \rho_d c_d / S_d$ for one-dimensional systems. In this case, it is also true that $\hat{p}_t = \hat{p}_d$. These results consequently affect Eq. (10).

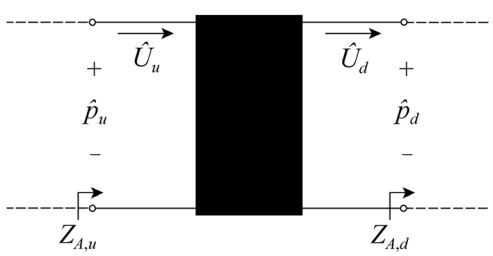

FIG. 6. Acoustic impedance circuit of an arbitrary black box (two-port network) separating an upstream (source) space and a downstream (receiving) space.

If the source and receiving spaces have identical characteristic impedances and cross-sectional areas, i.e., if $\rho_u c_u = \rho_d c_d = \rho_0 c$ and $S_u = S_d = S$, Eq. (10) simplifies to

$$\tau = \left|\frac{\hat{U}_d}{\hat{U}_u}\right|^2 \left|\frac{Z_{A,d} + \dfrac{\rho_0 c}{S}}{Z_{A,u} + \dfrac{\rho_0 c}{S}}\right|^2. \tag{11}$$

Both this expression and Eq. (10) may be easily applied to a variety of normal-incidence sound transmission problems

D. Normal-incidence transmission coefficient of a baffled loudspeaker

To explore the normal-incidence transmission coefficient of the baffled loudspeaker, we return to the analogous circuit in Fig. 4, incorporating the assumption that the frame and magnet structure are acoustically unobtrusive at all frequencies of interest. The circuit yields several useful relationships:

$$Z_{A,u} = \frac{Z_M}{S_D{}^2} + \frac{(Bl)^2}{(Z_E + Z_{ET})S_D{}^2} + Z_{ATT}, \tag{12}$$

$$Z_{A,d} = Z_{ATT}, \tag{13}$$

$$\hat{U}_u = \hat{U}_d = \hat{U}_D. \tag{14}$$

(If the filtering of the frame and magnet structure are to be considered, one must substitute Z'_{ATT} for Z_{ATT}.) Use of these relationships in Eq. (11) leads to the inverted transmission coefficient

$$\frac{1}{\tau} = \left|1 + \frac{Z_M + \dfrac{(Bl)^2}{(Z_E + Z_{ET})}}{Z_{ATT}S^2 + \rho_0 cS}\left(\frac{S}{S_D}\right)^2\right|^2. \tag{15}$$

As indicated earlier, several conditions may be considered for the electric test impedance Z_{ET}. If the driver terminals are open circuited, $Z_{ET} \to \infty$ and the inverted coefficient becomes

$$\frac{1}{\tau_{OC}} = \left|1 + \frac{Z_M}{Z_{ATT}S^2 + \rho_0 cS}\left(\frac{S}{S_D}\right)^2\right|^2. \tag{16}$$

If the driver terminals are closed circuited, $Z_{ET} \to 0$ and the inverted coefficient becomes

$$\frac{1}{\tau_{CC}} = \left|1 + \frac{Z_M + \dfrac{(Bl)^2}{Z_E}}{Z_{ATT}S^2 + \rho_0 cS}\left(\frac{S}{S_D}\right)^2\right|^2. \tag{17}$$

All three forms may be profitably compared to the inverted transmission coefficient for an ideal single-leaf partition (or ideal open-circuit loudspeaker) with cross-sectional area $S_D = S$ and an anechoic receiving tube termination ($Z_{ATT} = \rho_0 c/S$):[34,41]

$$\frac{1}{\tau_{SL}} = \left|1 + \frac{Z_M}{2\rho_0 cS}\right|^2. \tag{18}$$

III. NONANECHOIC DOWNSTREAM TERMINATIONS AND DECOMPOSITIONS OF DOWNSTREAM FIELDS

When Chung and Blaser introduced the concept of normal-incidence transmission loss measurements using the two-microphone transfer function technique,[29,30] they proposed an experimental arrangement involving both upstream and downstream microphone pairs for field decompositions. The downstream pair was included in the arrangement despite the presence of a supposedly anechoic receiving tube termination. The authors acknowledged the fact that nonanechoic terminations detrimentally impact measured data, but stated, "The anechoic end condition [was] not the requirement in the… method." Because no further explanation was given, one is left to question the rationale of their downstream measurement approach.

A passive anechoic termination typically falls short of producing ideal absorption at some frequencies. The absorption coefficient of a porous wedge-like termination progressively drops below 0.99 at frequencies below its anechoic "cutoff frequency." A downstream microphone pair might then be used to decompose the receiving tube field into the steady-state pressure components incident upon and reflected from the termination, allowing the incident component to act as the transmitted pressure. However, because transmission loss measurements inherently require the loading of an ideal anechoic receiving space,[42] one must question whether the downstream field decomposition really produces better experimental results or not. Is the pressure component incident upon the termination a better representation of the ideal transmitted pressure than the total downstream pressure itself? Would the use of the latter and a simple assumption of an anechoic termination make a difference for better or worse?

A. Analytical formulations

Consider the case of the open-circuit driver in the test system, with the inverted transmission coefficient given in Eq. (16). Constant upstream incident pressure and downstream pressure decomposition were used in the derivation of the expression. The result is theoretically equivalent to that produced by the two-microphone transfer function technique when both upstream and downstream microphone pairs are used to separate the incident (right-going) pressure components. Again, the component incident upon the receiving tube serves as the transmitted pressure.

How does this compare to the case in which one simply *assumes* the termination is anechoic then uses the total downstream pressure (i.e., without downstream decomposition) on the transmitting side of the driver as the transmitted pressure? The total pressure $\hat{p}_d = \hat{U}_D Z_{ATT}$ follows from Fig. 4. Using this for $\hat{p}_t$ in Eq. (9) leads to an alternative expression for the inverted transmission coefficient

TABLE I. Example properties of a loudspeaker driver, measurement system, and air within the measurement system.

Loudspeaker driver		Measurement system		Air	
Parameter	Value	Property	Value	Property	Value
Bl	3.10 T m	S	7.85×10^{-3} m^2	ρ_0	1.21 kg/m^3
C_{MS}	5.00×10^{-4} m/N	L_d	1.00 m	c	343 m/s
f_0	105 Hz	d	1.00 m	γ	1.402
L_E	0.300 mH	σ	0.95	η	1.85×10^{-5} Pa s
M_{MD}	4.58×10^{-3} kg	Ξ'	1000 kg/m^3 s	c_p	1.01×10^3 J/kg K
R_E	6.50 Ω			κ	0.0263 W/m K
R_{MS}	0.575 kg/s			Pr	0.710
S_D	5.30×10^{-3} m^2				

$$\frac{1}{\tau_{OC}} = \frac{1}{4}\left|1 + \frac{Z_M\left(\frac{S}{S_D}\right)^2 + \rho_0 c S}{Z_{ATT} S^2}\right|^2. \tag{19}$$

By way of comparison to this and Eq. (16), the correct expression (assuming a truly anechoic receiving field) is

$$\frac{1}{\tau_{OC}} = \left|1 + \frac{Z_M\left(\frac{S}{S_D}\right)^2}{2\rho_0 c S}\right|^2, \tag{20}$$

which follows directly from both Eqs. (16) and (19) when $Z_{ATT} = \rho_0 c/S$. When Z_{ATT} becomes larger than this, the first formulation in Eq. (16) tends to be too small, but the second formulation in Eq. (19) tends to be even smaller. When Z_{ATT} becomes smaller than this, the first expression tends to be too large, but the second expression tends to be even larger. This clearly suggests that the first formulation, involving both upstream and downstream field decompositions (as proposed by Chung and Blaser) tends to produce smaller measurement errors than the second approach. Interestingly, this result contradicts the assertion of other authors, who stated that the concept of downstream decomposition was simply erroneous.[46] However, the development here shows only one example related to specific plane-wave tube partitions. Additional exploration is required before a more general conclusion can be drawn.

B. Numerical example

A simple numerical example of a nonideal frequency-dependent termination impedance follows by assuming the termination is a porous layer of depth d and using the viscous Rayleigh model for porous materials to roughly characterize its behavior.[47] If the cross-sectional area of the termination is S, its acoustic impedance is approximately

$$Z_{AT} = -j\frac{\rho_0 c}{\sigma S}\left(1 - j\frac{\Xi'}{\rho_0 \omega}\right)^{1/2} \cot \tilde{k}'_m d, \tag{21}$$

where σ is the porosity, Ξ' is the specific flow resistance of a characteristic pore, and

$$\tilde{k}'_m = k\left(1 - j\frac{\Xi'}{\rho_0 \omega}\right)^{1/2} \tag{22}$$

is the complex acoustic wave number within the material. The pressure-amplitude reflection coefficient looking into the termination is then

$$R_T = \frac{Z_{AT} - \frac{\rho_0 c}{S}}{Z_{AT} + \frac{\rho_0 c}{S}}, \tag{23}$$

and the absorption coefficient is

$$\alpha_T = 1 - |R_T|^2. \tag{24}$$

Propagation losses over the length of the tube may also be addressed through the introduction of a complex wave number $\tilde{k} = k - j\alpha_p$, where α_p is the total propagation absorption (attenuation) coefficient.[48] However, for many practical tube lengths, cross-sectional areas, and terminations, the effects of these losses are negligible.

Table I lists several properties of a small driver and a plane-wave tube measurement system, including a nonideal absorptive termination. The frequency-dependent absorption coefficient of the termination is shown in Fig. 7. The ideal transmission loss of the driver (i.e., that evaluated with an ideal anechoic termination) and those resulting from Eqs.

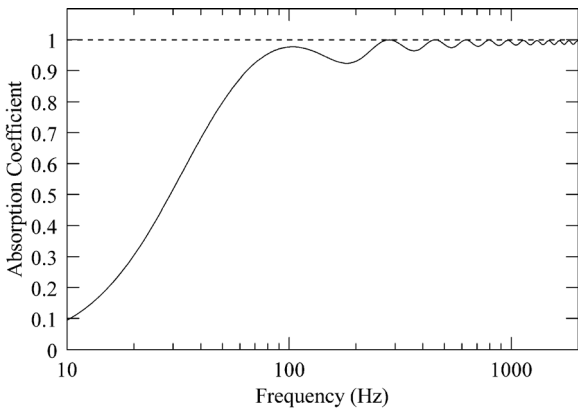

FIG. 7. Absorption coefficient of a hypothetical receiving tube termination for a plane-wave tube measurement system. Properties of the porous termination are listed in Table I.

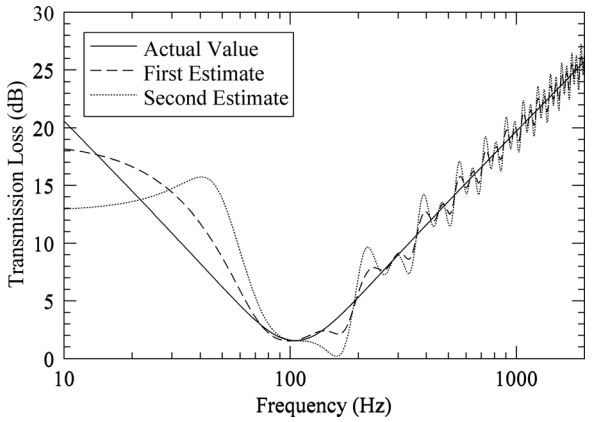

FIG. 8. Transmission loss of an open-circuit driver with parameters given in Table I. Two approximations to the transmission loss are plotted against the actual transmission loss (i.e., for an ideal anechoic receiving tube termination). The approximations result from a nonideal termination with the frequency-dependent absorption coefficient given in Fig. 7. The first approximation, based on Eq. (16), uses both upstream and downstream field decompositions. The second approximation, based on Eq. (19), uses only an upstream field decomposition and the total downstream pressure for the transmitted pressure.

(16) and (19) with the nonideal termination are given in Fig. 8. They include minor propagation losses in the tube. As suggested earlier, the first measurement formulation in Eq. (16) effectively involves both upstream (through a constant incident pressure source) and downstream field decompositions. It tends to produce smaller extremes in measurement error than the second formulation in Eq. (19), which involves the isolated upstream incident pressure and the total downstream pressure for the transmitted pressure. For either estimate, the figure demonstrates the likelihood of greater errors for frequencies with less absorption and the need to maintain the anechoic termination behavior to as low a frequency as possible. Despite the use of both upstream and downstream field decompositions, the presence of an anechoic receiving tube termination remains important.

The absorption of even a very deep, porous, wedge-like termination rolls off at sufficiently low frequencies (e.g., when its depth becomes small compared to wavelength). For drivers with very low resonance frequencies, the method could thus require a very long measurement apparatus. (For example, in preliminary measurements, the authors employed a 2.5 m resistive termination.[13,38]) Effective measurements can be made with these terminations, but if their lengths become problematic, the two-load method could provide a robust solution.[49,50] The latter enables the assessment of transmission coefficients that would have been measured under more ideal conditions using relatively short terminations. Resonant passive absorbers, hybrid passive absorbers, active absorbers, or hybrid active/passive absorbers could also be developed to provide good results.

IV. DERIVATION OF DRIVER PARAMETERS

Once successful transmission loss measurements have been conducted for open and closed-circuit driver conditions, various loudspeaker parameters can be derived from the transmission coefficients. The following sections provide the details of these derivations.

A. Resonance frequency

The inverted open-circuit transmission coefficient in Eq. (16) may be expanded as

$$\frac{1}{\tau_{OC}} = \frac{\left[\rho_0 cS + R_{ATT}S^2 + R_M\left(\frac{S}{S_D}\right)^2\right]^2 + \left[X_{ATT}S^2 + X_M\left(\frac{S}{S_D}\right)^2\right]^2}{(\rho_0 cS + R_{ATT}S^2)^2 + (X_{ATT}S^2)^2}. \tag{25}$$

If the receiving tube termination is truly anechoic or the transmission coefficient has been carefully measured with the two-load (or comparable) method (hereafter termed "ideal measurement conditions"), $R_{ATT} = \rho_0 c/S$ and $X_{ATT} = 0$ in the expression. After substituting these values, expanding the expression further, differentiating it with respect to frequency, and setting the result to zero, one finds the minimum of the inverted transmission coefficient, which corresponds to the *in vacuo* resonance frequency of the driver:

$$f_0 = \frac{1}{2\pi}\sqrt{\frac{1}{M_{MD}C_{MS}}}. \tag{26}$$

Under nonideal measurement conditions, the frequency corresponding to the minimum of the function will depend to some degree upon the termination impedance and may differ somewhat from this result. The effect is illustrated in Fig. 8, wherein the actual resonance frequency is 105.2 Hz and the estimated resonance frequency (corresponding to the minimum in the transmission loss for the first estimate) is 99.1 Hz. The obvious way to correct the discrepancy is to ensure ideal anechoic behavior in the vicinity of the resonance (or use an ideal implementation of the two-load or comparable method). However, computational tools, including curve-fitting routines, might also be used with for less ideal conditions to suitably estimate the resonance frequency.

B. Mechanical resistance of the suspension

Because the mechanical reactance of the driver diaphragm assembly vanishes at the resonance frequency, the mechanical resistance of the suspension follows from Eq. (25) as

$$R_{MS} = \left(\frac{S_D}{S}\right)^2 \left(\pm \left\{ \frac{1}{\tau_{OC,0}} \left[(\rho_0 c S + R_{ATT} S^2)^2 + (X_{ATT} S^2)^2 \right] - (X_{ATT} S^2)^2 \right\}^{1/2} - (\rho_0 c S + R_{ATT} S^2) \right), \tag{27}$$

where $\tau_{OC,0}$ is the transmission coefficient at resonance. In this expression and others that follow, the $\pm$ sign must be adapted to satisfy physical constraints. It is chosen here to ensure R_{MS} is positive. While the inclusion of R_{ATT} and X_{ATT} partially compensates for nonideal termination behavior (i.e., via downstream field decomposition), any error in the foregoing selection of f_0 can still lead to an error in $\tau_{OC,0}$, which may in turn produce some error in the value of R_{MS}. Under ideal measurement conditions, the expression reduces to

$$R_{MS} = 2\frac{\rho_0 c}{S} {S_D}^2 \left[\pm \left(\frac{1}{\tau_{OC,0}} \right)^{1/2} - 1 \right]. \tag{28}$$

C. Mechanical reactance, moving mass, and compliance of the diaphragm assembly

The frequency-dependent mechanical reactance of the diaphragm assembly may also be solved from Eq. (25) as

$$X_M = \left(\frac{S_D}{S}\right)^2 \left(\pm \left\{ \frac{1}{\tau_{OC}} \left[(\rho_0 c S + R_{ATT} S^2)^2 + (X_{ATT} S^2)^2 \right] - \left[\rho_0 c S + R_{ATT} S^2 + R_{MS} \left(\frac{S}{S_D} \right)^2 \right]^2 \right\}^{1/2} - X_{ATT} S^2 \right). \tag{29}$$

The mechanical resistance R_{MS} is first solved as outlined in the previous section then substituted into this formula. The $\pm$ sign is chosen in this case to ensure the reactance is negative below and positive above f_0. Under ideal measurement conditions, the expression reduces to the form

$$X_M = \pm \left(\frac{S_D}{S}\right)^2 \times \left\{ \frac{1}{\tau_{OC}} (2\rho_0 c S)^2 - \left[2\rho_0 c S + R_{MS} \left(\frac{S}{S_D} \right)^2 \right]^2 \right\}^{1/2}. \tag{30}$$

In both expressions, R_{MS} is assumed to remain constant over the measurement bandwidth.

The effective moving mass of the diaphragm assembly M_{MD} and the effective mechanical compliance of the suspension C_{MS} are related to one another through Eq. (26) and the mechanical reactance

$$X_M = \omega M_{MD} - \frac{1}{\omega C_{MS}}. \tag{31}$$

They may therefore be estimated through curve fitting or from asymptotic behaviors of the reactance curve at stiffness-controlled (low-frequency) and mass-controlled (high-frequency) extremes:

$$C_{MS} \approx \frac{1}{\omega X_{M,LF}} \tag{32}$$

$$M_{MD} \approx \frac{X_{M,HF}}{\omega}. \tag{33}$$

Values near the lowest and highest valid measurement frequencies may therefore be used (directly or through extrapolation) to approximate the two quantities. Equation (26) may subsequently be used to validate these values or produce one parameter after the other has been estimated. (Depending upon the characteristics of the driver and measurement system, one parameter may be easier to estimate using the asymptotic approach than the other.)

D. Force factor (*Bl* product)

The expression for the inverted closed-circuit transmission coefficient in Eq. (17) may be expanded as

$$\frac{1}{\tau_{CC}} = \frac{\left\{ \rho_0 c S + R_{ATT} S^2 + \left[R_{MS} + \frac{(Bl)^2 R_E}{R_E^2 + X_E^2} \right] \left(\frac{S}{S_D} \right)^2 \right\}^2 + \left\{ X_{ATT} S^2 + \left[X_M - \frac{(Bl)^2 X_E}{R_E^2 + X_E^2} \right] \left(\frac{S}{S_D} \right)^2 \right\}^2}{(\rho_0 c S + R_{ATT} S^2)^2 + (X_{ATT} S^2)^2}, \tag{34}$$

where R_E and X_E are the electric voice-coil resistance and reactance, respectively. The Bl product follows directly from this result as

$$Bl = \pm\left\{\left(\frac{S_D}{S}\right)^2\left[-\left(R_{ATT}S^2+\rho_0 cS+R_{MS}\left\{\frac{S}{S_D}\right\}^2\right)R_E+\left(X_M\left\{\frac{S}{S_D}\right\}^2+X_{ATT}S^2\right)X_E\right.\right.$$
$$\pm\left(\frac{1}{\tau_{CC}}\{[R_{ATT}S^2+\rho_0 cS]^2+[X_{ATT}S^2]^2\}\{R_E{}^2+X_E{}^2\}\right.$$
$$\left.\left.-\left\{\left[X_M\left(\frac{S}{S_D}\right)^2+X_{ATT}S^2\right]R_E+\left[R_{ATT}S^2+\rho_0 cS+R_{MS}\left(\frac{S}{S_D}\right)^2\right]X_E\right\}^2\right)^{1/2}\right]\right\}^{1/2}, \quad (35)$$

where the ± signs are selected to ensure Bl is real, positive, and relatively invariant over frequency. While the easily measurable R_E may be known, the frequency-dependent X_E may not be. Nevertheless, because it characteristically becomes very small in the low-frequency limit,

$$Bl \approx \pm\left\{R_E\left(\frac{S_D}{S}\right)^2\left[-\left(R_{ATT,LF}S^2+\rho_0 cS+R_{MS}\left\{\frac{S}{S_D}\right\}^2\right)\pm\left(\frac{1}{\tau_{CC}}\{[R_{ATT,LF}S^2+\rho_0 cS]^2+[X_{ATT,LF}S^2]^2\}\right.\right.\right.$$
$$\left.\left.\left.-\left\{X_{M,LF}\left[\frac{S}{S_D}\right]^2+X_{ATT,LF}S^2\right\}^2\right)^{1/2}\right]\right\}^{1/2}. \quad (36)$$

This expression is conveniently independent of X_E and under ideal measurement conditions reduces to the form

$$Bl \approx \pm\left\{R_E\left(\frac{S_D}{S}\right)^2\left[-\left(2\rho_0 cS+R_{MS}\left(\frac{S}{S_D}\right)^2\right)\pm\left(\frac{1}{\tau_{CC}}\{2\rho_0 cS\}^2-\left\{X_{M,LF}\left[\frac{S}{S_D}\right]^2\right\}^2\right)^{1/2}\right]\right\}^{1/2}. \quad (37)$$

E. Voice-coil inductance

Equation (34) may also be solved for X_E in terms of the force factor and other parameters:

$$X_E = \frac{1}{\beta}\left\{-(Bl)^2\left(\frac{S}{S_D}\right)^2\left[X_{ATT}S^2+X_M\left(\frac{S}{S_D}\right)^2\right]\pm\left(-(R_E\beta)^2+\left[(Bl)^2\left(\frac{S}{S_D}\right)^2\right]^2\left\{\beta+\left[X_{ATT}S^2+X_M\left(\frac{S}{S_D}\right)^2\right]^2\right\}\right.\right.$$
$$\left.\left.+2\left[R_{ATT}S^2+\rho_0 cS+R_{MS}\left(\frac{S}{S_D}\right)^2\right](Bl)^2\left(\frac{S}{S_D}\right)^2R_E\beta\right)^{1/2}\right\}, \quad (38)$$

where

$$\beta = \frac{1}{\tau_{CC}}[(X_{ATT}S^2)^2+(R_{ATT}S^2+\rho_0 cS)^2]-\left\{\left[R_{ATT}S^2+\rho_0 cS+R_{MS}\left(\frac{S}{S_D}\right)^2\right]^2+\left[X_{ATT}S^2+X_M\left(\frac{S}{S_D}\right)^2\right]^2\right\}. \quad (39)$$

Under ideal measurement conditions,

$$X_E = \frac{1}{\beta}\left\{-(Bl)^2\left(\frac{S}{S_D}\right)^2X_M\left(\frac{S}{S_D}\right)^2\pm\left(-(R_E\beta)^2+\left[(Bl)^2\left(\frac{S}{S_D}\right)^2\right]^2\left\{\beta+\left[X_M\left(\frac{S}{S_D}\right)^2\right]^2\right\}\right.\right.$$
$$\left.\left.+2\left[2\rho_0 cS+R_{MS}\left(\frac{S}{S_D}\right)^2\right](Bl)^2\left(\frac{S}{S_D}\right)^2R_E\beta\right)^{1/2}\right\}, \quad (40)$$

where

$$\beta = \frac{1}{\tau_{CC}}(2\rho_0 cS)^2-\left\{\left[2\rho_0 cS+R_{MS}\left(\frac{S}{S_D}\right)^2\right]^2+\left[X_M\left(\frac{S}{S_D}\right)^2\right]^2\right\}. \quad (41)$$

If the electric reactance is inductance controlled and the Bl product is known independently, the voice-coil inductance is simply

$$L_E = \frac{X_E}{\omega}. \tag{42}$$

The $\pm$ sign in Eqs. (38) and (40) are adapted to ensure L_E is positive. Since the classical model[11] of the blocked electric impedance $Z_E \approx R_E + j\omega L_E$ often provides an inadequate representation of its true frequency-dependent behavior, the method described herein could be applied (e.g., through curve fitting) to more advanced Z_E models, which might include semi-inductive and other effects.[51,52]

F. Numerical example

Consider again the hypothetical driver and measurement system described in Table I, with the nonideal termination absorption coefficient shown in Fig. 7. The preceding formulas and methods may be applied to the inverted transmission coefficient $1/\tau_{OC}$ (from the dashed transmission loss curve in Fig. 8) to predict the driver parameters as they would following an actual measurement. The formulations involving both upstream and downstream field decompositions produce more accurate parameter values than those based on the alternative formulations. The former are given in Table II, along with actual parameter values and percentage errors. In this example, M_{MD} was determined using the asymptotic high-frequency relationship in Eq. (33), but with a maximum simulated measurement frequency of 2 kHz (the approximate cutoff frequency of the first plane-wave tube cross mode) and no extrapolation. The value for L_E was determined from Eq. (42) at 1 kHz.

The errors for f_0 and R_{MS} would have been smaller had the receiving tube termination been more anechoic (or the two-load method been used) in the vicinity of the driver resonance frequency. However, curve fitting can improve the results without system modifications. In some cases, even a simple fit and calculation iteration can improve the outcome. For example, by using the asymptotically fitted C_{MS} and M_{MD} parameter values from Table II, one can reestimate f_0 using Eq. (26) and implement the result to recalculate R_{MS} using Eq. (27) and the original $1/\tau_{OC}$. Subsequent calculations yield little if any change to the estimated values of C_{MS} and M_{MD}, but they do improve those of Bl and L_E. As shown in Table III, this second calculation iteration provides parameter estimates that are consistently within 1% of the actual values. Thorough curve-fitting methods, such as those involving constrained optimization for functions of several variables, might incorporate parameter values from the first or second iteration as initial estimates then process the data to produce even more accurate results.

TABLE II. Estimated parameter values, actual parameter values, and rounded percentage errors for the simulated measurement of the loudspeaker driver described in Table I. The frequency-dependent inverted transmission coefficient (corresponding to the dashed transmission loss curve in Fig. 8) was used with the parameter formulations to produce these values.

Parameter	Estimated value	Actual value	Percentage error
Bl	3.14 T m	3.10 T m	1.3
C_{MS}	5.00×10^{-4} m/N	5.00×10^{-4} m/N	0.0
f_0	99.1 Hz	105.2 Hz	5.8
L_E	0.296 mH	0.300 mH	1.3
M_{MD}	4.57×10^{-3} kg	4.58×10^{-3} kg	0.3
R_{MS}	0.549 kg/s	0.575 kg/s	4.5

TABLE III. Estimated parameter values, actual parameter values, and rounded percentage errors for the simulated measurement of the loudspeaker driver described in Table I. In this case, f_0 was reestimated via Eq. (26) with C_{MS} and M_{MD} from Table II, then used to recalculate R_{MS} via Eq. (27). The results were used in subsequent calculations described in Sec. IV. This second calculation iteration yields greater accuracy in all estimates except those of C_{MS} and M_{MD}.

Parameter	Estimated value	Actual value	Percentage error
Bl	3.13 T m	3.10 T m	1.0
C_{MS}	5.00×10^{-4} m/N	5.00×10^{-4} m/N	0.0
f_0	105.3 Hz	105.2 Hz	0.1
L_E	0.298 mH	0.300 mH	0.7
M_{MD}	4.57×10^{-3} kg	4.58×10^{-3} kg	0.3
R_{MS}	0.576 kg/s	0.575 kg/s	0.2

While the parameter formulas appear to be frequency dependent, they should (in principle) produce correct values over frequency, including those that should be nearly constant. Of course, this is not exactly the case when prior estimation errors are present. Alternate $\pm$ signs are also required to satisfy physical constraints over frequency, but they can be chosen algorithmically according to the guidelines given throughout Sec. IV.

V. CONCLUSIONS

This paper has introduced the use of plane-wave tubes and normal-incidence transmission loss measurements to evaluate several classical parameters of moving-coil loudspeaker drivers. The method may also extend to more elaborate loudspeaker models and their parameters. It employs only acoustical excitation and measurement (no direct electrical excitation or measurement) and may thus be used to complement and validate existing electrical measurement techniques. It naturally extends to the evaluation of passive radiator parameters and could easily extend to the evaluation of other types of loudspeaker drivers (e.g., appropriately sized electrostatic drivers, planar magnetic drivers, etc.).

The measurement method is subject to systematic and random errors, as are other methods. This paper has explored one source of systematic error resulting from nonanechoic receiving tube terminations. Long, well-designed resistive terminations and downstream field decompositions can provide good measurement results. The two-load method would provide a robust solution with shorter terminations. The development and use of broadband anechoic terminations involving resonant or active elements could also be considered. Curve-fitting routines may be successfully employed with less ideal terminations and measurement methods to produce acceptable parameter values.

Other sources of error and their relationships to measurement accuracy and precision merit further investigation

and improvement. The use of upstream pressure-amplitude reflection coefficients has not been discussed in this paper, but it may prove useful for certain applications, including the measurement of drivers without open frames. We encourage exploration of these and other areas to refine the method and increase its utility.

[1]A. N. Thiele, "Loudspeakers in vented boxes: Parts I and II," Proc. IRE Australia **22**, 487–508 (1961) [reprinted in: J. Audio Eng. Soc. **19**, 382–392, 471–483 (1971)].

[2]J. E. Benson, "Theory and design of loudspeaker enclosures, Part 1.—Electroacoustical relations and generalized analysis," AWA Tech. Rev. **14**, 1–57 (1968).

[3]J. E. Benson, "Theory and design of loudspeaker enclosures, Part 2.—Response relationships for infinite-baffle and closed-box systems," AWA Tech. Rev. **14**, 225–293 (1971).

[4]J. E. Benson, "Theory and design of loudspeaker enclosures, Part 3.—Introduction to synthesis of vented systems," AWA Tech. Rev. **14**, 369–484 (1972).

[5]R. H. Small, "Direct-radiator loudspeaker system analysis," IEEE Trans. Audio Electroacoust. **19**, 269–281 (1971).

[6]R. H. Small, "Closed-box loudspeaker systems, Part I: Analysis," J. Audio Eng. Soc. **20**, 798–808 (1972).

[7]R. H. Small, "Closed-box loudspeaker systems, Part II: Synthesis," J. Audio Eng. Soc. **21**, 11–18 (1973).

[8]R. H. Small, "Vented-box loudspeaker systems, Part I: Small-signal analysis," J. Audio Eng. Soc. **21**, 363–372 (1973).

[9]R. H. Small, "Vented-box loudspeaker systems, Part II: Large-signal analysis," J. Audio Eng. Soc. **21**, 549–554 (1973).

[10]R. H. Small, "Vented-box loudspeaker systems, Part III: Synthesis," J. Audio Eng. Soc. **21**, 483–484 (1973).

[11]L. L. Beranek, *Acoustics* (Acoustical Society of America, New York, 1986), pp. 185–188, 211–230.

[12]J. C. Cox, "Comparison of loudspeaker driver parameter measurement techniques," *Proceedings of IMTC'85, IEEE Instrumentation and Measurement Technology Conference*, Tampa, FL (1985), pp. 254–258.

[13]B. E. Anderson, "Derivation of moving-coil loudspeaker parameters using plane wave tube techniques," M.S. thesis, Brigham Young University, 2003 [available online through Brigham Young University Electronic Theses & Dissertations at http://etd.lib.byu.edu (last viewed May 24, 2013)].

[14]J. Christophorou, "Low-frequency loudspeaker measurements with an accelerometer," J. Audio Eng. Soc. **28**, 809–816 (1980).

[15]J. N. Moreno, "Measurement of loudspeaker parameters using a laser velocity transducer and two-channel FFT analysis," J. Audio Eng. Soc. **39**, 243–249 (1991).

[16]D. Clark, "Precision measurement of loudspeaker parameters," J. Audio Eng. Soc. **45**, 129–141 (1997).

[17]E. Geddes, "Method for determining transducer linear operational parameters," U.S. Patent 6,269,318 (July 31, 2001).

[18]U. Seidel and W. Klippel, "Fast and accurate measurement of the linear transducer parameters," *110th Convention of the Audio Engineering Society*, Amsterdam (2001), Preprint 5308.

[19]V. K. Jain, W. M. Leach, and R. W. Schafer, "Time-domain measurement of vented-box loudspeaker system parameters," IEEE Trans. Acoust., Speech, Signal Process. **31**, 1–8 (1983).

[20]V. K. Jain, W. M. Leach, and R. W. Schafer, "Signal processing technique for measurement of vented-box loudspeaker system parameters," *Proceedings of ICASSP'82, IEEE Acoustics, Speech, and Signal Processing Conference*, Paris, France (1982), pp. 1428–1431.

[21]M. Ureda, "Determination of Thiele-Small parameters of a loudspeaker using nonlinear goal programming," *72nd Convention of the Audio Engineering Society*, Anaheim, CA (1982), Preprint 1953.

[22]Y. Nomura, T. Ai, and K. Fukuda, "Estimation method of direct-radiator loudspeaker system parameters in low-frequency range by nonlinear optimization technique," Electron. Commun. Jpn. **69**, 18–27 (1986) [translated from Denshi Tsushin Gakkai Ronbunshi **68-A**, 504–511 (1985)].

[23]M. H. Knudsen, J. G. Jensen, V. Julskjaer, and P. Rubak, "Determination of loudspeaker driver parameters using a system identification technique," J. Audio Eng. Soc. **37**, 700–708 (1989).

[24]W. Waldman, "Non-linear least squares estimation of Thiele-Small parameters from impedance measurements," *94th Convention of the Audio Engineering Society*, Berlin (1993), Preprint 3511.

[25]H. Jeong and J. Ih, "Harmonic balance method for estimating the nonlinear parameter of electrodynamic," J. Audio Eng. Soc. **44**, 245–257 (1996).

[26]J. Scott, J. Kelly, and G. Leembruggen, "New method of characterizing drive linearity," J. Audio Eng. Soc. **44**, 258–265 (1996).

[27]W. Klippel, "Measurement of large-signal parameters of electrodynamic transducer," *107th Convention of the Audio Engineering Society*, New York (1999), Preprint 5008.

[28]A. F. Seybert and D. F. Ross, "Experimental determination of acoustic properties using a two microphone random-excitation technique," J. Acoust. Soc. Am. **61**, 1362–1370 (1977).

[29]J. Y. Chung and D. A. Blaser, "Transfer function method of measuring in-duct acoustic properties. I. Theory," J. Acoust. Soc. Am. **68**, 907–913 (1980).

[30]J. Y. Chung and D. A. Blaser, "Transfer function method of measuring in-duct acoustic properties. II. Experiment," J. Acoust. Soc. Am. **68**, 914–921 (1980).

[31]H. Bodén and M. Åbom, "Influence of errors on the two-microphone method for measuring acoustic properties in ducts," J. Acoust. Soc. Am. **79**, 541–549 (1986).

[32]ASTM E1050-2012: *Standard Test Method for Impedance and Absorption of Acoustical Materials using a Tube, Two Microphones, and a Digital Frequency Analysis System* (ASTM International, West Conshohocken, PA, 2012).

[33]S. Riggs and E. Geddes, "A two microphone technique for the measurement of acoustic waveguide impedance," *87th Convention of the Audio Engineering Society*, New York (1989), Preprint 2878.

[34]T. W. Leishman, "Active control of sound transmission through partitions composed of discretely controlled modules," Ph.D. thesis, The Pennsylvania State University, 2000.

[35]T. W. Leishman and J. Tichy, "A theoretical and numerical analysis of vibration-controlled modules for use in active segmented partitions," J. Acoust. Soc. Am. **118**, 1424–1438 (2005).

[36]T. W. Leishman and J. Tichy, "An experimental investigation of two module configurations for use in active segmented partitions," J. Acoust. Soc. Am. **118**, 1439–1451 (2005).

[37]T. W. Leishman and J. Tichy, "An experimental investigation of two active segmented partition arrays," J. Acoust. Soc. Am. **118**, 3050–3063 (2005).

[38]B. E. Anderson and T. W. Leishman, "An acoustical measurement method for the derivation of loudspeaker parameters," *115th Convention of the Audio Engineering Society*, New York (2003), Preprint 5865.

[39]W. P. Mason, *Electromechanical Transducers and Wave Filters* (Van Nostrand, New York, 1942), pp. 204–205.

[40]J. L. Flanagan, *Speech Analysis Synthesis and Perception*, 2nd ed. (Springer-Verlag, Berlin, 1972), Chap. III.

[41]A. D. Pierce, *Acoustics: An Introduction to its Physical Principles and Applications* (Acoustical Society of America, New York, 1989), pp. 119–120, 140–143, 319–330, 351–354.

[42]F. Fahy, *Foundations of Engineering Acoustics* (Academic Press, London, 2001), pp. 201–202.

[43]P. M. Morse and K. U. Ingard, *Theoretical Acoustics* (Princeton University Press, Princeton, NJ, 1968), pp. 471–499.

[44]I. L. Vér and C. I. Holmer, "Interaction of sound waves with solid structures," in *Noise and Vibration Control*, revised edition, edited by L. L. Beranek (Institute of Noise Control Engineering, Washington, DC, 1988), p. 281.

[45]M. L. Munjal, *Acoustics of Ducts and Mufflers, with Application to Exhaust and Ventilation System Design* (John Wiley and Sons, New York, 1987), p. 58.

[46]Z. Tao and A. F. Seybert, "A review of current techniques for measuring muffler transmission loss," SAE Technical Paper No. 2003-01-1653 (2003).

[47]H. Kuttruff, *Room Acoustics*, 5th ed. (Spon Press, London, 2009), pp. 177–188.

[48]L. E. Kinsler, A. R. Frey, A. B. Coppens, and J. V. Sanders, *Fundamentals of Acoustics*, 4th ed. (Wiley, New York, 2000), Chap. 8, pp. 273, 277–280.

[49]T. Y. Lung and A. G. Doige, "A time-averaging transient testing method for acoustic properties of piping systems and mufflers," J. Acoust. Soc. Am **73**, 867–876 (1983).

[50]O. Olivieri, J. S. Bolton, and T. Yoo, "Measurement of transmission loss of materials using a standing wave tube," *Proceedings of Inter-Noise 2006*, Honolulu, HI (2006), Paper 374.

[51]K. Thorborg and A. D. Unruh, "Electrical equivalent circuit model for dynamic moving-coil transducers incorporating a semi-inductor," J. Audio Eng. Soc. **56**, 696–709 (2008).

[52]C. J. Struck, "ZFIT: A MATLAB tool for Thiele-Small parameter fitting and optimization," *129th Convention of the Audio Engineering Society*, San Francisco (2010), Preprint 8220.